Published in final edited form as:

ACS Nano. 2017 June 27; 11(6): 5367–5374. doi:10.1021/acsnano.7b01926.

Nanomotor-Enabled pH-Responsive Intracellular Delivery of Caspase-3: Towards Rapid Cell Apoptosis

Berta Esteban-Fernández de Ávila[†], **Doris E. Ramírez-Herrera**[†], **Susana Campuzano**[§], **Pavimol Angsantikul**[†], **Liangfang Zhang**[*,†], and **Joseph Wang**[*,†]

[†]Department of Nanoengineering, University of California, San Diego, La Jolla, California 92093, United States

[§]Department of Analytical Chemistry, Complutense University of Madrid, E-28040 Madrid, Spain

Abstract

Direct and efficient intracellular delivery of enzymes to cytosol holds tremendous therapeutic potential while remaining an unmet technical challenge. Herein, an ultrasound (US)-propelled nanomotor approach and a high pH-responsive delivery strategy is reported to overcome such challenge using caspase-3 (CASP-3) as a model enzyme. Consisting of a gold nanowire (AuNW) motor with a pH-responsive polymer coating, in which the CASP-3 is loaded, the resulting nanomotor protects the enzyme from release and deactivation prior to reaching an intracellular environment. However, upon entering a cell and exposure to the higher intracellular pH, the polymer coating is dissolved, thereby directly releasing the active CASP-3 enzyme to the cytosol and causing rapid cell apoptosis. *In vitro* studies using gastric cancer cells as a model cell line demonstrates that such motion-based active delivery approach leads to remarkably high apoptosis efficiency within significantly shorter time and lower amount of CASP-3 compared to other control groups without involving US-propelled nanomotors. For instance, the reported nanomotor system can achieve 80% apoptosis of human gastric adenocarcinoma (AGS) cells within only 5 min, which dramatically outperforms other CASP-3 delivery approaches. These results indicate that the US-propelled nanomotors may act as a powerful vehicle for cytosolic delivery of active therapeutic proteins, which would offer an attractive means to enhance the current landscape of intracellular protein delivery and therapy. While CASP-3 is selected as a model protein in this study, the same nanomotor approach can be readily applied to a variety of different therapeutic proteins.

Table of Contents Graphic

[*]**Corresponding Authors**. josephwang@ucsd.edu and zhang@ucsd.edu.

ASSOCIATED CONTENT

Supporting Information

Supporting videos description, supporting figures, and supporting table. This material is available free of charge *via* the Internet at http://pubs.acs.org.

Author Contributions

The manuscript was written through contributions of all authors. All authors have given approval to the final version of the manuscript.

The authors declare no competing financial interest.

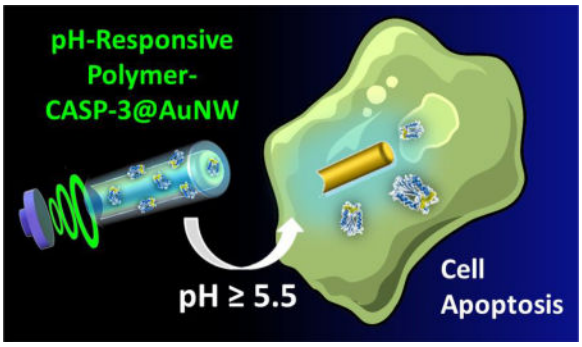

Keywords

nanomotor; caspase-3; apoptosis; pH-responsive polymer; ultrasound; intracellular delivery

INTRODUCTION

Considerable progress has been made recently towards the development of synthetic nano/micromachines with attractive capabilities for diverse biomedical applications,[1–3] including biosensing,[4–6] cargo delivery,[7–9] nanosurgery,[10,11] and detoxification.[12,13] The attractive movement, cargo-towing, and navigation functions of different self-propelled and externally-powered nano/micromotors[1,14–18] have led to their growing use for active transport and delivery of therapeutic payloads, compared to common diffusion-based passive approaches.[19–23] Nano/microscale machines have thus demonstrated promise for improving the diagnosis and treatment of cancer by delivering anticancer drugs to specific target sites,[7,20,24,25] isolating circulating tumor cells,[26] monitoring intracellular miRNA expression,[6] or silencing specific genes inside cancer cells.[27]

Herein we describe a nanomotor-based apoptotic strategy involving the use of caspase-3 (CASP-3)-modified nanowire motors for rapid and efficient cell apoptosis. This approach represents the first example of using nanomotors for efficient intracellular delivery of a functional therapeutic enzyme. While intracellular delivery of functional proteins offers tremendous therapeutic potential,[28,29] the difficulty of rapid cytosolic delivery of proteins in active conformation is massive and still represents an unmet challenge.[30,31]

CASP-3 is a highly promising therapeutic protein.[28,32,33] This cysteine protease catalyzes the specific cleavage of key cellular proteins and thus plays a crucial role in programmed cell death (apoptosis).[34] Intracellular delivery of sufficient levels of active CASP-3 into the cytosol of target cells can induce the cells to undergo apoptosis by cleaving essential substrates[35] while minimizing side effects to healthy tissues and cells associated with current therapeutics.[28,32,33] Moreover, since the native form of CASP-3 is an endogenous cell component that requires external stimuli to activate it,[36] the delivery of a functionally active form of this enzyme obviates side effects and toxicity issues associated with external stimuli such as the use of chemical and radioactive therapeutics for inducing targeted cell apoptosis. However, the intracellular delivery of active CASP-3 enzyme is extremely challenging, due to its negative charge, heterotetrameric state, and the fragile nature of its

active site.[28] Although some promising strategies have been described so far for intracellular delivery of CASP-3, based on the use of lipid[37] or poly(disulfide)s[38] mediated mechanisms, and different nanovehicles[28,39,40] or delivery reagents,[41,42] most of them relied on complex protocols and required long incubation times and high amounts of the apoptotic enzyme.

In this sense, ultrasound (US)-powered nanowire motors represent a particularly attractive platform to overcome biological barriers and physical limitations associated to conventional methods for functional protein internalization,[27] in order to develop a simple and efficient strategy for intracellular delivery of CASP-3. The present nanomotor-based apoptosis strategy relies on the accelerated intracellular delivery of active CASP-3, encapsulated within a biocompatible pH-responsive polymeric coating on US-propelled gold nanowire (AuNW) motors. The commercial pH-responsive polymer Eudragit® L30 D-55 was selected for encapsulating CASP-3 enzyme, due to its rapid dissolution above pH 5.5,[43] thus ensuring safe arrival of the active enzyme to the intracellular environment while preventing the CASP-3 release in the extracellular space. The high pH-responsive CASP-3 delivery strategy was selected taking into account the gastric tumor microenvironment and the pH values found in malignant tumor cells, characterized by acidic (5.5–6.8) extracellular space and neutral (7.3–7.8) intracellular cytosol.[44,45] It should be pointed out also that while the new proof-of-concept has been demonstrated here for intracellular delivery in gastric cancer cells, a major goal of this study is to demonstrate the unique ability of the US-powered motors for intracellular delivery of therapeutic proteins. The new concept could thus be readily carried out using different cells and pH-responsive coatings, depending on the specific application.[46]

RESULTS AND DISCUSSION

As shown in Figure 1A, the AuNW motors were synthetized by a common membrane-template electrodeposition protocol (see Methods section), consisted of electrodeposition of gold (Figure 1A(a)) within the nanopores of an alumina membrane, followed by dissolution of the membrane and release of the resulting AuNWs. Subsequently, a droplet of the AuNWs was dispersed onto a glass slide until dried (Figure 1A(b)), and the wires were then coated with the pH-responsive polymeric layer containing CASP-3 enzyme (Figure 1A(c)). After the polymer/CASP-3 film was completely dried, the polymer/CASP-3 coated AuNW motors (denoted polymer/CASP-3@AuNWs) were collected by softly scratching the glass slide (Figure 1A(d)).

Figure 1B schematically illustrates the accelerated cell apoptosis process through *in situ* CASP-3 delivery using US-propelled nanomotors. The actual time-lapse image Figure 1C (middle panel, taken from Supporting Video S1) illustrates that the polymer/CASP-3-coated AuNW motors move under an US field, approaching a target cell. Upon entering the cell, the nanomotors are subject to intracellular pH environment (pH > 5.5), leading to dissolution of their pH-sensitive coating and concomitant release of active CASP-3 enzyme, which subsequently induces rapid cell apoptosis (Figure 1C, right panel). Compared to earlier approaches for intracellular CASP-3 delivery,[28,37–42] our nanomotor-based apoptotic strategy offers the highest apoptosis efficiency using significantly shorter time and a lower amount of CASP-3 (see comparison in Table S1 in the Supporting Information). As a proof

of concept, these advantages of the nanomotor-based apoptosis approach have been demonstrated using human gastric adenocarcinoma (AGS) cells, which are resistant to pH changes, and have been demonstrated to retain high viability at pH as low as 5.0.[47] The present polymer coating is expected to ensure the enzyme stability in the highly acidic gastric fluid of the stomach during potential *in vivo* gastric CASP-3 delivery applications. Our results indicate that the US-propelled nanomotors represent an attractive platform for effective delivery of active therapeutic enzymes to the cytosol of cells.

Scanning electron microscopy (SEM) imaging was carried out to examine the structural morphology of the AuNW motors. Figure 2A(a) displays an SEM image of an uncoated AuNW, showing the wire structure of the nanomotor with a 200 nm diameter, which reflects the pore size of the alumina membrane template. Figure 2A(b) and Figure 2B(a) show SEM images of a polymer/CASP-3@AuNW motor that illustrate the polymer/enzyme coating along the nanomotor structure (according to the schematic illustration of Figure 2A(c)). The diameter of the coated nanomotors is estimated from these images to be 280±8 nm, indicating an average coating thickness of ~40 nm. It is important to mention that the acoustic propulsion mechanism relies on US streaming over the rigid gold surface of the asymmetric AuNW, which contains a concave end (Figure 2B(a)) essential for the motion.[48] Although good results were obtained with the 4 μm-long polymer/CASP-3@AuNWs, the size and shape of the nanomotors could be further investigated in order to optimize the enzymatic loading and the apoptosis efficiency. The presence of Au, C, and N (from the motor core, polymer, and enzyme, respectively) was confirmed from the corresponding energy dispersive X-ray spectroscopy (EDX) mapping shown in Figure 2B(b–d). The US-propulsion of the polymer/CASP-3@AuNW motors was compared to that of uncoated AuNWs, as illustrated from the time-lapse images of Figure 2C(a) and 2C(b), respectively, and from Supporting Video S2. The polymer/CASP-3@AuNWs displayed efficient propulsion when compared to uncoated AuNWs, yielding average speeds of 37 and 47 μm/s, respectively (Figure 2C(c)). Such behavior indicates that coating of the motors with the polymer/CASP-3 film has a small effect upon their propulsion speed. Such fast movement is essential for achieving efficient internalization of the polymer/CASP-3@AuNWs into the cells. In practical *in vivo* applications, the 37 μm/s speed of the polymer/CASP-3@nanomotors would be sufficient to penetrate within few seconds the mucus layer of the stomach (~100 μm thickness) to reach and penetrate into the cancer cells, thus ensuring negligible enzymatic release in the extracellular space.

Prior to demonstrating the *in vitro* cell apoptosis induced by the polymer/CASP-3@AuNWs, the enzymatic loading yield of the nanomotors was quantified by using a commercial CASP-3 activity assay. Such assay relies on measuring the production of a CASP-3-dependent luminescent signal (as described in Methods section). Initially, a luminescence intensity calibration plot was constructed using different concentrations of pure CASP-3 (Figure S1). Subsequently, AuNWs were loaded with CASP-3 following the protocol earlier described. The loaded CASP-3 was released *in vitro* by increasing the solution pH from 5.0 to 7.0, thus ensuring complete dissolution of the polymer and the consequent release of the enzyme. After separating the nanomotors, the supernatant containing the released enzyme was analyzed with the commercial CASP-3 assay kit. The loading yield of the enzyme was then calculated by interpolating the luminescence intensity of the released CASP-3 into the

CASP-3 calibration plot. The estimated CASP-3 loading yield of 3.4 ng per batch of 6×10^5 motors was obtained, which was considered optimal to induce apoptosis also by other researchers.[37] This loading yield was thus used for all the experiments.

The morphology of AGS cells treated with US-propelled polymer/CASP-3@AuNWs and with different control conditions was examined before and after 1 h treatment. Figure 3 displays optical microscope images of AGS cells exposed to such different treatment conditions. Clear changes in the cell morphology, indicative of cell apoptosis (*i.e.*, irregular shape with blebs),[49] were observed after treating the cells with US-propelled polymer/CASP-3@AuNWs, as compared to the untreated AGS cells (Figure 3A *vs.* Figure 3F). A morphological change was also observed when treating cells with the free solution-phase CASP-3, with or without an US field (Figures 3B and 3C, respectively). On the other hand, negligible morphological changes of the AGS cells were observed following treatment with static polymer/CASP-3@AuNWs (Figure 3D), which demonstrates the important role of the US-propulsion to enable effective internalization of the nanomotors by the cells. Also, no apparent morphological changes were observed using cells treated with US field alone (Figure 3E).

Different control experiments were carried out to further confirm the role and performance of the US-propelled polymer/CASP-3@AuNWs in rapidly inducing cell apoptosis. This study involved evaluation of the AGS cell viability using a commercial cell proliferation spectrophotometric assay based on a MTS tetrazolium compound (Figure 4), following the protocol described in Method section. The measured absorbance values and the estimated apoptosis efficiency (%) are shown in Figures 4A and Figure 4B, respectively. The corresponding optical images of the cells in all the conditions assayed are displayed in Figure S2. All the control experiments were compared to untreated AGS cells (negative control, bar a), and to AGS cells treated with 2% Triton X-100 (positive control, bar j). An initial control experiment, carried out using only US indicated minor apoptosis efficiency (bar b). The non-acute cell toxicity found when using US-powered polymer-coated AuNWs (Figure 4B, bar c) is in agreement with previous results demonstrating that the same type of motors do not affect significantly the viability of the target cells.[50,51] In agreement with the qualitative observations of the cell morphology experiments, the highest apoptosis efficiency was observed using US-powered polymer/CASP-3@AuNWs. These coated nanomotors resulted in 80.0% apoptosis efficiency, which is 3.3-times higher than the 24.4% efficiency observed with the static ones (Figure 4B: bars i *vs.* d). Such dramatic enhancement of the apoptosis efficiency demonstrates the important role of US-propulsion in the CASP-3 induced apoptosis process. Moreover, the 80.0% apoptosis achieved using US-propelled polymer/CASP-3@AuNWs, compared with the 36.1% apoptosis using free CASP-3 released from the motor under the same US conditions (Figure 4B: bars i *vs.* h), demonstrates the significant role of AuNWs in cytosolic delivery of CASP-3. On the other hand, a similar apoptosis efficiency was observed using the same amount of free CASP-3 in solution and CASP-3 released *in vitro* from the motors, either under static conditions (31.0% *vs* 30.1%, Figure 4B: bars f and e, respectively) or US condition (36.1% *vs* 35.7%, Figure 4B: bars h and g, respectively). Overall, these results demonstrate the high efficacy of the presented intracellular protein delivery approach using pH-responsive polymer-coated AuNWs. The data shows that CASP-3 maintains its activity after immobilization on the

motors using the commercial pH-responsive polymer. Caspases are delicate enzymes that are susceptible to inactivation during delivery process,[28] but these results reflect the protective action of the pH-responsive polymer and indicate their stability throughout the nanomotor-based delivery process. While the exact reason of this stability is not fully understood, it could be attributed to the entrapment of the enzyme within the polymer coating that retains a stable CASP-3 structure similar to that observed by other researchers after its confinement in polyethyleneglycol.[52]

Overall, compared with other apoptosis approaches reported to date (Table S1), this nanomotor strategy results in the highest apoptosis efficiency while using significantly shorter times and smaller amounts of CASP-3. The dramatically faster apoptosis and lower amounts of CASP-3 reflect the movement of the US-propelled AuNWs and their efficient delivery of active CASP-3 to the cytosol of target cells, and the CASP-3 stability in the pH-responsive polymer. A magnetic segment could be easily incorporated into the US-propelled polymer/CASP-3@AuNWs, which allows the motors to be easily and specifically guided to the cancerous tissue, limiting the apoptosis strictly to the target cancer cells and minimizing the toxicity evoked to normal cells.

CONCLUSIONS

We have demonstrated that the combination of synthetic nanomotors with apoptotic enzyme CASP-3 enabled direct and rapid intracellular protein delivery with significantly enhanced cell apoptosis efficacy and efficiency compared to other delivery approaches. Specifically, these US-propelled CASP-3 delivery nanomotors could be rapidly internalized into cancer cells and dramatically improve the apoptosis efficiency compared with static nanomotors or free enzyme-based approaches using similar CASP-3 levels. Up to 80% apoptosis of AGS cells has been observed after 5 min treatment with US-propelled high-pH responsive polymer/CASP-3@AuNWs. Such improvement reflects the necessity and importance of fast internalization and rapid intracellular movement of nanomotors for effective cytosolic protein delivery. A series of control experiments supported the important role of the nanomotor movement in the efficient induction of apoptosis, and of the high-pH responsive polymer in ensuring the functional activity of the delivered enzyme. Although such nanomotor-based intracellular delivery approach is still in its infancy and further system optimization is required for in vivo drug delivery to gastric tumor, this initial proof-of-concept *in vitro* study clearly indicates that US-propelled nanomotors may act as an efficient vehicle for direct cytosolic delivery of active therapeutic proteins. It should be pointed out that while a high-pH responsive polymer has been used in the present study as a coating for intracellular protein delivery in gastric cancer cells, different pH-responsive coatings could be readily used for specific applications, based on the corresponding extracellular/intracellular pH conditions.

METHODS

Reagents and solutions

The commercial pH-responsive coating (enteric polymer Eudragit® L30 D-55) was obtained from Evonik Industries (Germany).

Active Recombinant Human Caspase-3, (CASP-3, 5 μg, 37.5 KDa) was purchased from BioVision, Inc. (Milpitas, CA). The lyophilized CASP-3 was reconstituted in phosphate buffer saline (PBS) solution pH 7.4 containing 15% glycerol. The enzyme was divided into 90 nM aliquots, and immediately stored at −70°C until use. Standard solutions of the enzyme were prepared daily from the 90 nM stored aliquots in the same buffer solution.

AGS cells (human gastric adenocarcinoma, ATCC® CRL-1739™) were cultured in Ham's F-12K medium (Gibco) supplemented with 10% fetal calf serum (Hyclone), penicillin-streptomycin (Gibco) at 37 °C in a humidified atmosphere containing 5% CO_2. Before the experiments, cell cultures were detached with 0.25% trypsin-EDTA (Gibco) and resuspended in fresh cell culture media. Concentrations of cells in suspension were measured by hemocytometer (Hausser Scientific Partnership, Horsman, PA) and adjusted to 5×10^4 cells/mL by cell culture media.

All chemicals used were of analytical-grade reagents, and deionized water was obtained from a Millipore Milli-Q purification system (18.2 MΩ cm at 25 °C).

Nanomotors fabrication

The gold nanowire (AuNW) motors were prepared by a common template-directed electrodeposition protocol. A thin gold film was first sputtered on one side of the porous alumina membrane template containing 200-nm diameter cylindrical nanopores (Catalogue No. 6809-6022; Whatman, Maidstone, UK) to serve as a working electrode. The membrane was assembled in a Teflon plating cell with aluminum foil serving as an electrical contact for the subsequent electrodeposition. A sacrificial copper layer was electrodeposited into the branched area of the membrane using a 1 M cupric sulfate pentahydrate solution ($CuSO_4.5H_2O$, Sigma-Aldrich, St. Louis, MO), using a charge of 8 C and a potential of −0.90 V (*vs* a Ag/AgCl reference electrode, along with a Pt-wire as a counter electrode). The removal of this sacrificial layer helped to create the concave shape in one end of the gold wire nanomotor. Subsequently, Au was plated using a commercial gold plating solution (Orotemp 24 RTU RACK; Technic Inc., Anaheim, CA) at −0.95 V (*vs* Ag/AgCl), using a charge of 3.5 C. The resulting AuNWs had a length of around 4 μm. The sputtered gold layer and the copper sacrificial layer were simultaneously removed by mechanical polishing using cotton tip applicators soaked with 0.5 M $CuCl_2$ solution in 20% HCl. The membrane was then dissolved in a 3 M NaOH solution for 30 min to completely release the nanowires. The resulting nanomotors were separated from solution by centrifugation at 7,000 rpm for 5 min and washed repeatedly with ultrapure water (18.2 MΩ cm) until a neutral pH was achieved. Between washing steps, the nanomotors solution was mixed with ultrapure water and briefly sonicated (3 s) to ensure complete dispersion of nanomotors in the washing water. All AuNWs were stored in 1 mL of ultrapure water at room temperature until use.

CASP-3 loading onto nanomotors

The commercial Eudragit® L30 D-55 enteric polymer was chosen to be loaded with CASP-3 enzyme and to be coated on the AuNW motors to prevent the release of CASP-3 from the nanomotors in the extracellular environment, thus ensuring the safe arrival of the active enzyme to the intracellular space. First, a batch of AuNWs (~6×10^5 motors) was collected in

water, and the micromotor suspension was dispersed onto a glass slide and let it until dried. The CASP-3-loaded nanomotors were prepared by using a mixture of Eudragit® L30 D-55 polymer and 90 nM CASP-3 solution. The nanomotors were coated with a 100 μL film of the enzyme-polymer mix solution. Finally, after the enzymatic-polymeric film was completely evaporated, the pH-responsive-polymer-CASP-3@AuNWs were collected in a 1.5 mL tube by lightly scratching the motors off the glass slide. It is worth to mention that no significant aggregation of the AuNW motors or any loss of CASP-3 activity was observed using this modification protocol. All steps were carried out at room temperature.

pH-responsive polymer-coated AuNWs without CASP-3 were also prepared using the same protocol to perform the corresponding control experiments.

The polymeric-enzyme coating thickness was examined by SEM. The 200 nm original diameter of the nanomotors (defined by the micropores of the alumina membrane template) was compared with the 280±8 nm coated-nanomotors, calculating an average coating thickness of ~80 nm.

Quantification of CASP-3 loading yield

To estimate the CASP-3 loading on the nanomotors, a luminescent assay that measures caspase-3 activity (Caspase-Glo® 3/7 Assay; Promega Corporation) was used. First, a luminescence intensity calibration plot using different concentrations of pure CASP-3 was constructed (Figure S1), being the luminescent signal proportional to the amount of caspase activity. Then, AuNWs were loaded with CASP-3 following the protocol described above. After that, the loaded CASP-3 was *in vitro* released by increasing the pH of the solution from 5.0 to 7.0, thus ensuring the complete dissolution of the polymer and the consequent release of the enzyme. After separate the nanomotors, the supernatant containing the released enzyme was mixed with the Caspase-Glo® 3/7 reagent following the specifications of the commercial kit. Luminometer readings were taken after 1 hour incubation at room temperature. The luminescence intensity of the released CASP-3 was interpolated into the luminescence intensity calibration plot, from which the loading yield of enzyme was calculated. The estimated CASP-3 loading yield was 3.4 ng per batch of motors (average value based on the values calculated from 3 different batches of motors).

In vitro intracellular apoptosis induction

The nanomotor-based cell apoptosis induction mechanism involved the *in vitro* apoptosis induction of AGS cells by the intracellular CASP-3 released from the pH-responsive polymer-CASP-coated nanomotors. To perform these experiments, a mixture of 2.5 μL of the cell suspension (~600 cells/μL) and 2.5 μL of the pH-responsive polymer-CASP-3@AuNWs (~6×10^5 motors) was prepared and put into the US holder, applying 6 V and 2.56 MHz during 5 min. After performing 3 incubations, the total volume (~5.0×10^3 cells) of the mixture solution was placed in a well containing 90 μL Corning cellar DMEM media (pH adjusted to 5.0) with 4.5 g/L glucose, L-glutamine, and sodium pyruvate; 10% Hylcone Bovine Growth Serum (FBS); and 1% penicillin streptomycin. The pH value of the media was selected taking into account the gastric tumor microenvironment and the pH

values found in malignant tumor cells, characterized by acidic (5.5–6.8) extracellular space and neutral (7.3–7.8) intracellular cytosol.[44]

Cell viability/apoptosis assay

To determine the apoptosis efficiency, cell viability was assessed using the CellTiter 96® AQueous One Solution Cell Proliferation Assay (Promega Corporation), based on a MTS tetrazolium compound. In brief, 10 μL of the MTS reagent were added into each well (containing the mix of nanomotors and cells), mixed gently, and incubated at 37 °C for 3 h. This was followed by reading the absorbance of the 96 well-plate at 490 nm using a plate reader. The quantity of formazan product as measured by Abs at 490 nm was directly proportional to the number of living cells. The percentage of apoptosis was calculated assuming that the average absorbance of the wells containing non-treated cells represented 100% viability.

Ultrasound equipment

The acoustic cell setup consisted of a piezoelectric transducer (Ferroperm PZ26 disk 10 mm diameter, 0.5 mm thickness) responsible for the generation of ultrasound waves, attached by conductive epoxy glue to the bottom center of a steel plate (50 mm × 50 mm × 0.94 mm^3); then the steel plate was covered with a 240 μm kapton tape protective layer and a sample reservoir at the center (5 mm). A glass slide was used to cover the reservoir for ultrasound reflection and to protect the sample. The continuous ultrasound sine wave was applied *via* a piezoelectric transducer, through an Agilent 15 MHz arbitrary waveform generator, in connection to a home-made power amplifier. The applied continuous sine wave form had a frequency of 2.56 MHz and 6 V voltage amplitude.

Videos were captured using Cool SNAP HQ^2 camera, 20× and 40× objectives (unless mentioned otherwise) and acquired at the frame rate of 10 using the Metamorph 7.1 software (Molecular Devices, Sunnyvale, CA). A Nikon Eclipse 80i upright microscope was also used to capture time course images of the morphological changes of AGS cells treated with US-propelled pH-responsive polymer-CASP-3@nanomotors and other conditions.

Supplementary Material

Refer to Web version on PubMed Central for supplementary material.

Acknowledgments

This work was supported by the Defense Threat Reduction Agency Joint Science and Technology Office for Chemical and Biological Defense (Grant Numbers HDTRA1-13-1-0002 and HDTRA1-14-1-0064) and by the National Cancer Institute of the National Institutes of Health (Award Number R01CA200574). Doris E. Ramírez-Herrera acknowledges a doctoral fellowship from CONACYT.

References

1. Wang, J. Nanomachines: Fundamentals and Applications. Wiley-VCH; Weinheim, Germany: 2013.
2. Li J, Esteban-Fernández de Ávila B, Gao W, Zhang L, Wang J. Micro/Nanorobots for Biomedicine: Delivery, Surgery, Sensing, and Detoxification. Sci. Robot. 2017:2. eaam6431.

3. Wang J, Gao W. Nano/Microscale Motors: Biomedical Opportunities and Challenges. ACS Nano. 2012; 6:5745–5751. [PubMed: 22770233]
4. Kagan D, Campuzano S, Balasubramanian S, Kuralay F, Flechsig GU, Wang J. Functionalized Micromachines for Selective and Rapid Isolation of Nucleic Acid Targets from Complex Samples. Nano Lett. 2011; 11:2083–2087. [PubMed: 21491941]
5. Orozco J, Campuzano S, Kagan D, Zhou M, Gao W, Wang J. Dynamic Isolation and Unloading of Target Proteins by Aptamer-Modified Microtransporters. Anal. Chem. 2011; 83:7962–7969. [PubMed: 21888314]
6. Esteban-Fernández de Ávila B, Martin A, Soto F, Lopez-Ramirez MA, Campuzano S, Vásquez Machado GM, Gao W, Zhang L, Wang J. Single Cell Real-Time miRNAs Sensing Based on Nanomotors. ACS Nano. 2015; 9:6756–6761. [PubMed: 26035455]
7. Wu Z, Wu Y, He W, Lin X, Sun J, He Q. Self-Propelled Polymer-Based Multilayer Nanorockets for Transportation and Drug Release. Angew. Chem., Int. Ed. 2013; 52:7000–7003.
8. Felfoul O, Mohammadi M, Taherkhani S, de Lanauze D, Xu YZ, Loghin D, Essa S, Jancik S, Houle D, Lafleur M, et al. Magneto-Aerotactic Bacteria Deliver Drug-Containing Nanoliposomes to Tumour Hypoxic Regions. Nat. Nano. 2016; 11:941–947.
9. Huang TY, Sakar MS, Mao A, Petruska AJ, Qiu F, Chen XB, Kennedy S, Mooney D, Nelson BJ. 3D Printed Microtransporters: Compound Micromachines for Spatiotemporally Controlled Delivery of Therapeutic Agents. Adv. Mater. 2015; 27:6644–6650. [PubMed: 26415002]
10. Kagan D, Benchimol MJ, Claussen JC, Chuluun-Erdene E, Esener S, Wang J. Acoustic Droplet Vaporization and Propulsion of Perfluorocarbon-Loaded Microbullets for Targeted Tissue Penetration and Deformation. Angew. Chem., Int. Ed. 2012; 51:7519–7522.
11. Chatzipirpiridis G, Ergeneman O, Pokki J, Ullrich F, Fusco S, Ortega JA, Sivaraman KM, Nelson BJ, Pané S. Electroforming of Implantable Tubular Magnetic Microrobots for Wireless Ophthalmologic Applications. Adv. Healthcare Mater. 2015; 4:209–214.
12. Wu Z, Li T, Gao W, Xu T, Jurado-Sánchez B, Li J, Gao W, He Q, Zhang L, Wang J. Cell-Membrane-Coated Synthetic Nanomotors for Effective Biodetoxification. Adv. Funct. Mater. 2015; 25:3881–3887.
13. Wu Z, Li J, Esteban-Fernández de Ávila B, Li T, Gao W, He Q, Zhang L, Wang J. Water-Powered Cell-Mimicking Janus Micromotor. Adv. Funct. Mater. 2015; 25:7497–7501.
14. Wang H, Pumera M. Emerging Materials for the Fabrication of Micro/Nanomotors. Nanoscale. 2017; 9:2109–2116. [PubMed: 28144663]
15. Wang W, Duan W, Ahmed S, Mallouk TE, Sen A. Small Power: Autonomous Nano- and Micromotors Propelled by Self-Generated Gradients. Nano Today. 2013; 8:531–554.
16. Wang H, Pumera M. Fabrication of Micro/Nanoscale Motors. Chem. Rev. 2015; 115:8704–8735. [PubMed: 26234432]
17. Sánchez S, Soler L, Katuri J. Chemically Powered Micro- and Nanomotors. Angew. Chem., Int. Ed. 2015; 54:1414–1444.
18. Kim K, Guo J, Xu X, Fan DL. Recent Progress on Man-Made Inorganic Nanomachines. Small. 2015; 11:4037–4057. [PubMed: 26114572]
19. Cheng R, Huang W, Huang L, Yang B, Mao L, Jin K, Zhu GQ, Zhao Y. Acceleration of Tissue Plasminogen Activator-Mediated Thrombolysis by Magnetically Powered Nanomotors. ACS Nano. 2014; 8:7746–7754. [PubMed: 25006696]
20. Xuan M, Shao J, Lin X, Dai L, He Q. Self-Propelled Janus Mesoporous Silica Nanomotors with Sub-100 nm Diameters for Drug Encapsulation and Delivery. Chem. Phys. Chem. 2014; 4:2255–2260.
21. Gao W, Dong R, Thamphiwatana S, Li J, Gao W, Zhang L, Wang J. Artificial Micromotors in the Mouse's Stomach: A Step toward *in Vivo* Use of Synthetic Motors. ACS Nano. 2015; 9:117–123. [PubMed: 25549040]
22. Gao W, Wang J. Synthetic Micro/Nanomotors in Drug Delivery. Nanoscale. 2014; 6:10486–10494. [PubMed: 25096021]
23. Peng F, Tu Y, van Hest JC, Wilson DA. Self-Guided Supramolecular Cargo-Loaded Nanomotors with Chemotactic. Angew. Chem., Int. Ed. 2015; 54:11662–11665.

24. Garcia-Gradilla V, Sattayasamitsathit S, Soto F, Kuralay F, Yardımcı C, Wiitala D, Galarnyk M, Wang J. Ultrasound-Propelled Nanoporous Gold Wire for Efficient Drug Loading and Release. Small. 2014; 10:4154–4159. [PubMed: 24995778]
25. Wu Z, Lin X, Wu Y, Si T, Sun J, He Q. Near-Infrared Light-Triggered "On/Off" Motion of Polymer Multilayer Rockets. ACS Nano. 2014; 8:6097–6105. [PubMed: 24806430]
26. Balasubramanian S, Kagan D, Hu C-MJ, Campuzano S, Lobo-Castañon MJ, Lim N, Kang DY, Zimmerman M, Zhang L, Wang J. Micromachine-Enabled Capture and Isolation of Cancer Cells in Complex Media. Angew. Chem., Int. Ed. 2011; 50:4161–4164.
27. Esteban-Fernández de Ávila B, Angell C, Soto F, Lopez-Ramirez MA, Báez DF, Xie S, Wang J, Chen Y. Acoustically Propelled Nanomotors for Intracellular siRNA Delivery. ACS Nano. 2016; 10:4997–5005. [PubMed: 27022755]
28. Tang R, Kim CS, Solfiell DJ, Rana S, Mout R, Velázquez-Delgado EM, Chompoosor A, Jeong Y, Yan B, Zhu ZJ, et al. Direct Delivery of Functional Proteins and Enzymes to the Cytosol Using Nanoparticle-Stabilized Nanocapsules. ACS Nano. 2013; 7:6667–6673. [PubMed: 23815280]
29. Fu A, Tang R, Hardie J, Farkas ME, Rotello VM. Promises and Pitfalls of Intracellular Delivery of Proteins. Bioconjugate Chem. 2014; 25:1602–1608.
30. Gu Z, Biswas A, Zhao M, Tang Y. Tailoring Nanocarriers for Intracellular Protein Delivery. Chem. Soc. Rev. 2011; 40:3638–3655. [PubMed: 21566806]
31. Yan L, Zhang J, Lee CS, Chen X. Micro- and Nanotechnologies for Intracellular Delivery. Small. 2014; 10:4487–4504. [PubMed: 25168360]
32. Raff M. Cell Suicide for Beginners. Nature. 1998; 396:119–122. [PubMed: 9823889]
33. Thornberry NA, Lazebnik Y. Caspases: Enemies Within. Science. 1998; 281:1312–1316. [PubMed: 9721091]
34. Porter AG, Jänicke RU. Emerging Roles of Caspase-3 in Apoptosis. Cell Death Differ. 1999; 6:99–104. [PubMed: 10200555]
35. De la Torre C, Mondragon L, Coll C, García-Fernández A, Sancenón F, Martínez-Máñez R, Amorós P, Pérez-Payá E, Orzáez M. Caspase 3 Targeted Cargo Delivery in Apoptotic Cells Using Capped Mesoporous Silica Nanoparticles. Chem. Eur. J. 2015; 21:15506–15510. [PubMed: 26493876]
36. Cho KC, Jeong JH, Chung HJ, Joe CO, Kim SW, Park TG. Folate Receptor-Mediated Intracellular Delivery of Recombinant Caspase-3 for Inducing Apoptosis. J. Control. Release. 2005; 108:121–131. [PubMed: 16139916]
37. Zelphati O, Wang Y, Kitada S, Reed JC, Felgner PL, Corbeil J. Intracellular Delivery of Proteins with a New Lipid-Mediated Delivery System. J. Biol. Chem. 2001; 276:35103–35110. [PubMed: 11447231]
38. Fu J, Yu C, Li L, Yao SQ. Intracellular Delivery of Functional Proteins and Native Drugs by Cell-Penetrating Poly(disulfide)s. J. Am. Chem. Soc. 2015; 137:12153–12160. [PubMed: 26340272]
39. Cheng Q, Blais MO, Harris G, Jabbarzadeh E. PLGA-Carbon Nanotube Conjugates for Intercellular Delivery of Caspase-3 into Osteosarcoma Cells. PLoS One. 2013; 8:e81947. [PubMed: 24312611]
40. Li Y, Li P, Zhu R, Luo C, Li H, Hu S, Nie Z, Huang Y, Yao S. Multifunctional Gold Nanoclusters-Based Nanosurface Energy Transfer Probe for Real-Time Monitoring of Cell Apoptosis and Self-Evaluating of Pro-Apoptotic Theranostics. Anal. Chem. 2016; 88:11184–11192. [PubMed: 27778512]
41. Zassler B, Blasig IE, Humpel C. Protein Delivery of Caspase-3 Induces Cell Death in Malignant C6 Glioma, Primary Astrocytes and Immortalized and Primary Brain Capillary Endothelial Cells. J. Neurooncol. 2005; 71:127–134. [PubMed: 15690127]
42. Postupalenko V, Desplancq D, Orlov I, Arntz Y, Spehner D, Mely Y, Klaholz BP, Schultz P, Weiss E, Zuber G. Protein Delivery System Containing a Nickel-Immobilized Polymer for Multimerization of Affinity-Purified His-Tagged Proteins Enhances Cytosolic Transfer. Angew. Chem., Int. Ed. 2015; 54:10583–10586.
43. Hales D, Iovanov RI, Achim M, Leucuţa SE, Muntean D, Vlase L, Tomuţă I. Development of a pH and Time Controlled Release Colon Delivery System Obtained by Compression-Coating and Film-Coating. Pharmacy. 2015; 63:510–517.

44. Fais S. Proton Pump Inhibitor-Induced Tumour Cell Death by Inhibition of a Detoxification Mechanism. J. Intern. Med. 2010; 267:515–525. [PubMed: 20433578]

45. Tannock IF, Rotin D. Acid pH in Tumors and Its Potential for Therapeutic Exploitation. Cancer Res. 1989; 49:4373–4384. [PubMed: 2545340]

46. Li J, Thamphiwatana S, Liu W, Esteban-Fernández de Ávila B, Angsantikul P, Sandraz E, Wang J, Xu T, Soto F, Ramez V, et al. Enteric Micromotor Can Selectively Position and Spontaneously Propel in the Gastrointestinal Tract. ACS Nano. 2016; 10:9536–9542.

47. Yeo M, Kim DK, Kim YB, Oh TY, Lee JE, Cho SW, Kim HC, Hahm KB. Selective Induction of Apoptosis with Proton Pump Inhibitor in Gastric Cancer Cells. Clin. Cancer Res. 2004; 10:8687–8696. [PubMed: 15623654]

48. Rao KJ, Li F, Meng L, Zheng H, Cai F, Wang W. A Force to Be Reckoned With: A Review of Synthetic Microswimmers Powered by Ultrasound. Small. 2015; 11:2836–2846. [PubMed: 25851515]

49. Kothakota S, Azuma T, Reinhard C, Klippel A, Tang J, Chu K, McGarry TJ, Kirschner MW, Koths K, Kwiatkowski DJ, et al. Caspase-3–Generated Fragment of Gelsolin: Effector of Morphological Change in Apoptosis. Science. 1997; 278:294–298. [PubMed: 9323209]

50. Ahmed S, Wang W, Mair LO, Fraleigh RD, Li S, Castro LA, Hoyos M, Huang TJ, Mallouk TE. Steering Acoustically Propelled Nanowire Motors toward Cells in a Biologically Compatible Environment Using Magnetic Fields. Langmuir. 2013; 29:16113–16118. [PubMed: 24345038]

51. Wang W, Li S, Mair L, Ahmed S, Huang TJ, Mallouk TE. Acoustic Propulsion of Nanorod Motors Inside Living Cells. Angew. Chem., Int. Ed. 2014; 53:3201–3204.

52. Ishimoto T, Jigawa K, Henares TG, Sueyoshi K, Endo T, Hisamoto H. Efficient Immobilization of the Enzyme and Substrate for a Single-Step Caspase-3 Inhibitor Assay Using a Combinable PDMS Capillary Sensor Array. RSC Adv. 2014; 4:7682–7687.

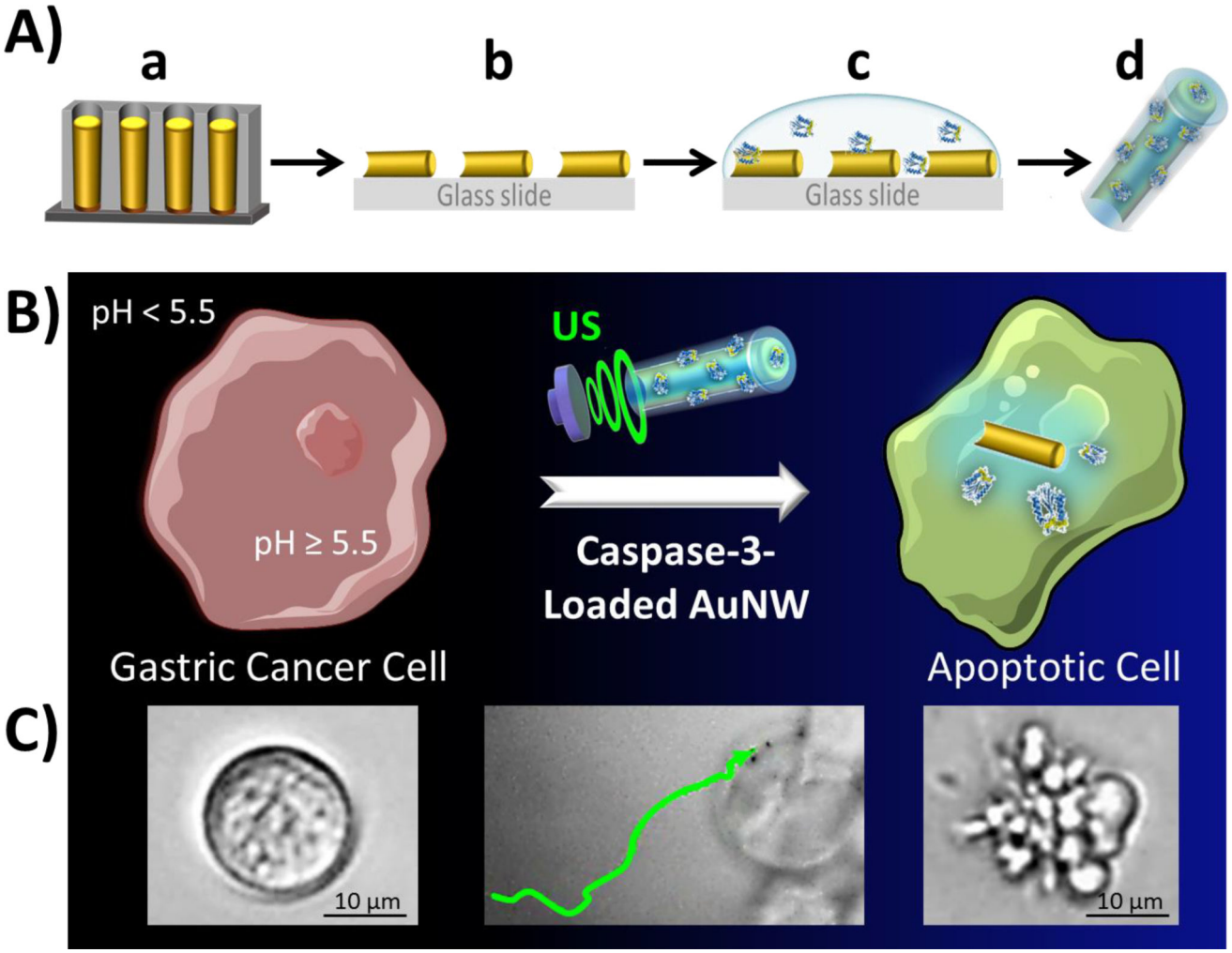

Figure 1. Preparation of pH-responsive polymer/CASP-3 coated AuNW motors (polymer/CASP-3@AuNWs) and their intracellular delivery of CASP-3

(A) Schematic preparation of the polymer/CASP-3@AuNWs: template electrodeposition of AuNWs (a), release of AuNWs from the nanoporous alumina membrane and AuNWs dispersion over a glass slide (b), coating AuNWs with a CASP-3-loaded pH-responsive polymer (c), and release of the polymer/CASP-3 coated AuNWs by a soft scratching of the glass slide (d). (B) Schematic of the nanomotor-based CASP-3 intracellular delivery to induce apoptosis of the recipient cell: the polymer/CASP-3@AuNW enters a cell through US-enabled active motion; upon entering the cell, the pH-responsive polymer coating dissolves, releasing the enzyme and inducing cell apoptosis. (C) Actual time-lapse images of a healthy AGS cell, US-powered polymer/CASP-3@AuNWs approaching an AGS cell, and an apoptotic AGS cell (from left to right, respectively).

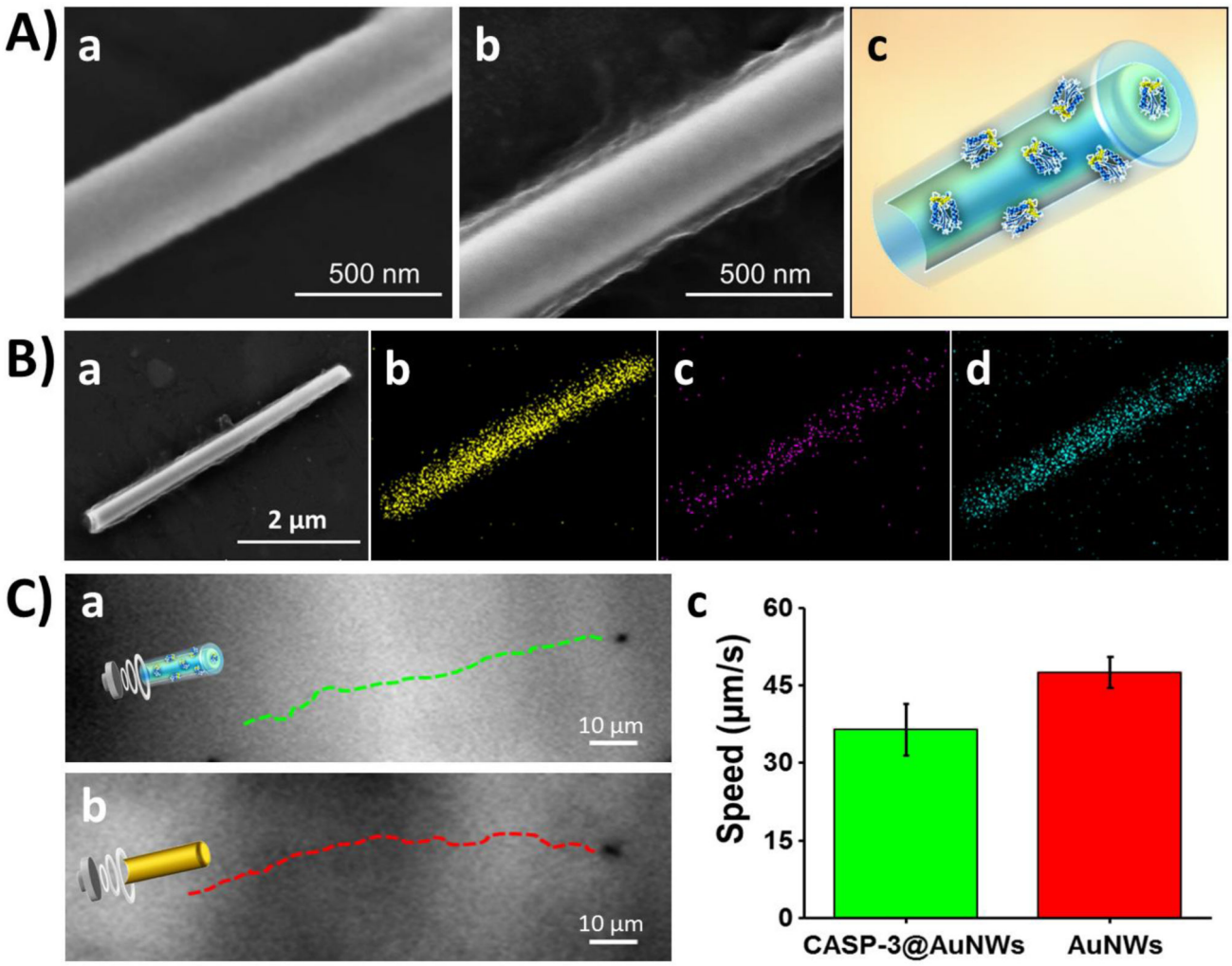

Figure 2. Characterization of the polymer/CASP-3@AuNWs

(A) Comparison of scanning electron microscopy (SEM) images of an uncoated AuNW (a) and a polymer/CASP-3@AuNW (b), along with a schematic image of the polymer/CASP-3@AuNW motor (c). (B) SEM image of a polymer/CASP-3@AuNW motor (a), and corresponding energy-dispersive X-ray spectroscopy (EDX) images showing the distribution of gold (b), carbon (c), and nitrogen (d). (C) Time-lapse optical images, taken from Supporting Video S2, showing the propulsion behavior of a polymer/CASP-3@AuNW motor (a) and an uncoated AuNW motor (b); (c) comparison of the speed of the US-powered polymer/CASP-3@AuNW motors (green bar) and uncoated AuNW motors (red bar). US field: 6 V, 2.56 MHz.

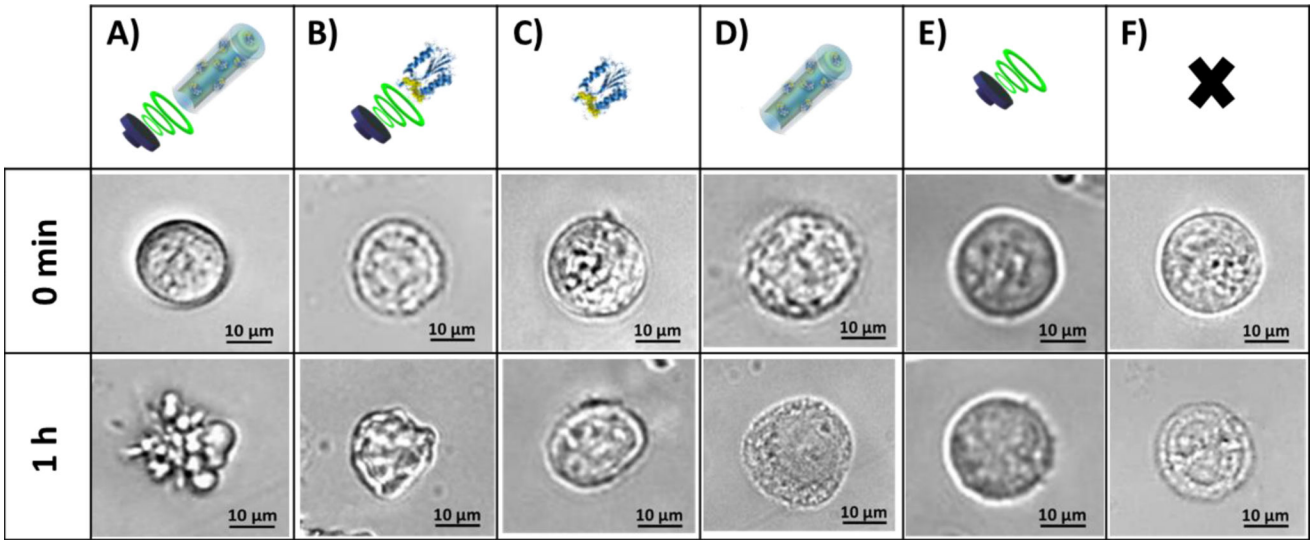

Figure 3. Evaluation of the morphological changes of AGS cells treated with US-propelled polymer/CASP-3@AuNW motors or with other control conditions

Comparison of optical microscope images taken at different times (0 min and 1 h) of AGS cells treated with: US-propelled polymer/CASP-3@AuNWs (A), 3.4 ng of free CASP-3 and applying US (B), 3.4 ng of free CASP-3 without US (C), polymer/CASP-3@AuNWs without US (D), US alone (E), and untreated AGS cells (F, used as a negative control).

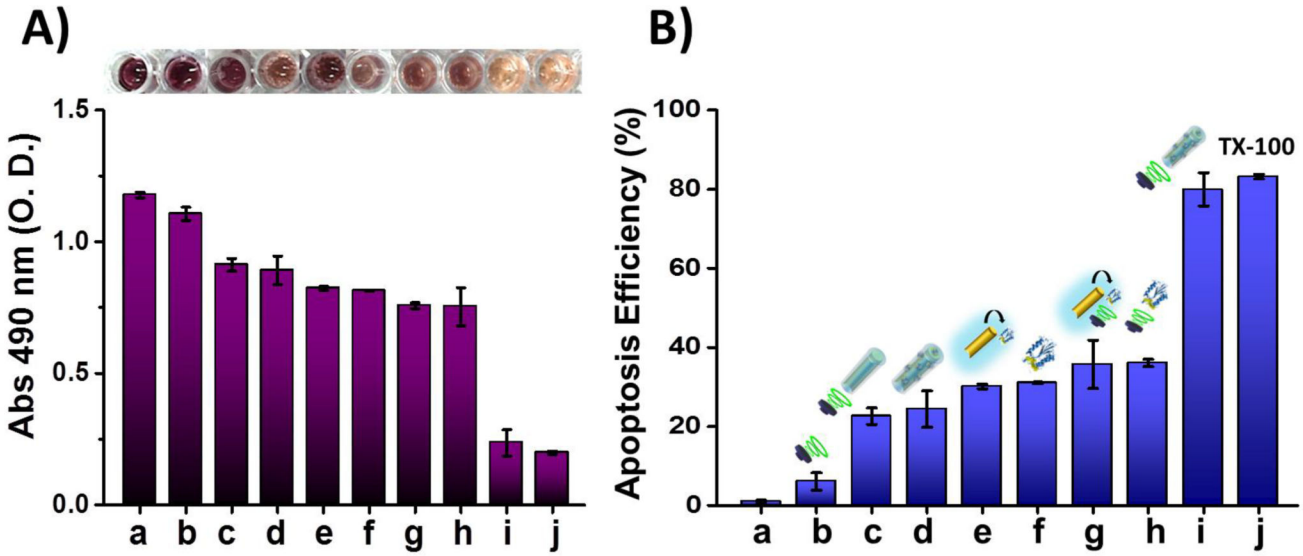

Figure 4. Apoptosis of gastric cancer cells induced by polymer/CASP-3@AuNW motors along with control experiments

(A) MTS cytotoxicity assay results. Absorbance measured at 490 nm from cells incubated under different conditions: untreated cells (a), cells only treated with US (b), cells treated with US-powered polymer coated AuNWs (no CASP-3) (c), cells treated with static polymer/CASP-3@AuNWs (no US) (d), cells treated with CASP-3 released from motors and static conditions (e), cells treated with same amount of free CASP-3 under static conditions (f), cells treated with CASP-3 released from motors and US conditions (g), cells treated with same amount of free CASP-3 under US conditions (h), cells treated with US-powered polymer/CASP-3@AuNWs (i), and cells treated with 2% Triton X-100 used as a positive control (j). All cells were incubated with the MTS reagent at 37°C for 3 h before measuring the corresponding absorbance. (B) Bar diagram illustrating the cell apoptosis efficiency observed in the different treatment groups. US conditions: 6 V, 2.56 MHz and 5 min. Other conditions: 110 μL total solution volume; 6×10^5 nanomotors; 5×10^3 AGS cells; 3.4 ng of CASP-3; Dulbecco's Modified Eagle Medium (DMEM).